

EUROPEAN ORGANIZATION FOR NUCLEAR RESEARCH  
European Laboratory for Particle Physics



INFN, Torino

**Internal Note/**

ALICE reference number

ALICE-INT-2005-041 version 1.0

Institute reference number

[-]

Date of last change

15th December 2005

## Reconstruction of decay vertices of strange particles in pp collisions in ALICE

### Authors:

Ludovic Gaudichet\*  
For the ALICE Collaboration

### Abstract:

In this note we examine the capability of ALICE to reconstruct  $K_s^0$  and hyperons in pp collisions. Event selection criteria as well as suitable selection parameters for  $K_s^0$ ,  $\Lambda$ ,  $\Xi$  and  $\Omega$  are presented. More than 120000 Monte-Carlo pp events have been simulated by the PYTHIA event generator and then fully reconstructed with the ALICE reconstruction software. The results allow us to determine the  $\Lambda$  and  $\Xi$  reconstruction rates associated to our selection parameters as a function of the transverse momentum. Predictions of  $\Lambda$ ,  $\Xi$  and  $\Omega$  raw yields as a function of  $p_t$  are finally made for the first year of run at the LHC.

---

\* gaudichet@to.infn.it

# Reconstruction of decay vertices of strange particles in pp collisions in ALICE

Ludovic Gaudichet\*

15th December 2005

INFN - Istituto Nazionale di Fisica Nucleare, Torino (Italy)

## Abstract

In this note we examine the capability of ALICE to reconstruct  $K_S^0$  and hyperons in pp collisions. Event selection criteria as well as suitable selection parameters for  $K_S^0$ ,  $\Lambda$ ,  $\Xi$  and  $\Omega$  are presented. More than 120000 Monte-Carlo pp events have been simulated by the PYTHIA event generator and then fully reconstructed with the ALICE reconstruction software. The results allow us to determine the  $\Lambda$  and  $\Xi$  reconstruction rates associated to our selection parameters as a function of the transverse momentum. Predictions of  $\Lambda$ ,  $\Xi$  and  $\Omega$  raw yields as a function of  $p_t$  are finally made for the first year of run at the LHC.

## 1 Introduction

The ALICE experiment [1] is dedicated to the study of the quark gluon plasma (QGP) created in ultra-relativistic heavy ion collisions. It is therefore specifically designed for the reconstruction of the Pb-Pb collisions of 5.5 TeV produced at the LHC. However, ALICE will also participate in the study of pp collisions, where the reconstruction of strange particles will be very useful as we will see in the following.

As a matter of fact the LHC will provide elementary collisions first. Thus the analysis of the production of strange particles in pp collisions will prepare the analysis in Pb-Pb collisions, both from the technical and the physics points of view. For numerous observables the understanding of the specific behaviours of A-A collisions can be understood only in comparison with the data from lighter systems and especially pp. For instance at the top SPS energies the comparison between the yields of strange and multi-strange hyperons in Pb-Pb collisions and the same yields in smaller colliding systems (e.g. pp, pBe) led to the observation of the so-called strangeness enhancement [2]. If this effect was firstly suggested to be one more evidence of deconfinement [3], it was later interpreted simply in terms of canonical suppression due to the small system size obtained with pp collisions. This can be qualitatively reproduced by thermal models [4] and dynamically by transport models [5]. However, there are still open questions at LHC energies: 1) what would be the correlated volume describing properly the system with respect to strange particle production [6] and/or the scale ruling strange quark production [7]; 2) will the differences be still significant between Pb-Pb and pp collisions. In the hypothesis that deconfinement could eventually occur in pp collisions as well [8], strange production analysis may give the first insight of it.

One of the major results at RHIC has been the clear evidence of high transverse momentum suppression and jet quenching phenomenon [9, 10]. In this field of research, reconstruction of secondary vertices and strange particles may shed light on flavour dependence of in-medium effects as well as jet suppression since no limit in momentum other than statistics is reached using this identification method. Corresponding analysis must be performed both for pp and Pb-Pb data before concluding.

Measurements in elementary collisions will not only establish references for the heavy-ion analysis at LHC but can in themselves bring significant insights into the pp collisions. Understanding pp physics at LHC will require the study of all phenomena, including the processes with large cross-section and ALICE can provide significant contributions and results in this sector. In many respects, strangeness studies can play an important role in the determination of the general properties of pp collisions. First of all, they will allow to shed light on baryon production mechanisms at LHC energies. It has been proposed that gluons could carry a part of the baryon number [11, 12] and in such a case, baryon stopping would not simply be a mechanical process and

---

\*gaudichet@to.infn.it

would extend to mid-rapidity. Mid-rapidity measurements of the baryon asymmetry for protons and  $\Lambda$  would clearly reveal this phenomenon. Equations 1 and 2 show the expressions of these asymmetries as well as their corresponding values if this hypothesis [13] is valid :

$$A_p = 2 \frac{p - \bar{p}}{p + \bar{p}} \approx 0.05, \quad (1)$$

$$A_\Lambda = 2 \frac{\Lambda - \bar{\Lambda}}{\Lambda + \bar{\Lambda}} \approx 0.3. \quad (2)$$

The mean transverse momentum ( $\langle p_t \rangle$ ) in pp collisions is also not well understood : when observed at RHIC as a function of the particle mass [14, 15], the  $\langle p_t \rangle$  for the heavy particles tends to approach the values obtained in Au–Au collisions. Whereas transverse radial flow increases the observed  $\langle p_t \rangle$  of particles in heavy ion collisions, the reasons of similar values for pp collisions remain uncertain. Two other examples show that strangeness is a key tool for investigating the properties of pp collisions: 1) strange baryon production allows to address the flavour dependence of the fragmentation functions [16]; 2) the feed-down correction of proton yield needs the measurement of the primary  $\Lambda$  yield which in turns require the measurement of  $\Xi$ .

In this note we show that the statistics of the first year of data taking at the LHC (estimated to be  $10^9$  pp events) should allow to determine the main characteristics of hyperon production at mid-rapidity in elementary collisions. Studies of  $\Lambda$  and  $K_S^0$  and of  $\Xi^-$  and  $\Omega^-$  production in pp collisions at mid-rapidity and with the ALICE detector are presented.

More than 120000 Monte Carlo events have been generated with the PYTHIA event generator [17]. These simulations allowed us to determined the expected reconstruction rates in pp for neutral single strange particles ( $K_S^0$ ,  $\Lambda$ ) and charged multi-strange ones ( $\Xi$ ,  $\Omega$ ). The invariant mass distributions, the reconstruction rates as a function of  $p_t$  as well as the  $p_t$  spectra for a typical year of LHC running are also presented. Finally we will discuss the assumptions we used for these studies and the physics points which will be investigated.

## 2 Simulation and selection strategies

The topological methods implemented for the reconstruction of strange particles [18] in Pb–Pb events are also used for  $V^0$  vertices and cascades identification in pp events. The cut parameters are however relaxed in order to obtain the same signal to background ratio. One additional selection is made by requiring that a given track can be associated to one  $V^0$  and one cascade only. Thus, only the best candidate is kept when several  $V^0$  or cascades have a common track.

The reconstruction of secondary vertices relies on the reconstruction of the primary vertex. In contrast with Pb–Pb events, the primary vertex resolution in pp varies over a wide range as a function of the multiplicity and can be considerably worse than the value obtained in Pb–Pb collisions. Typically the resolution is of the order of  $150 \mu m$  at high multiplicity while it can be worse than  $400 \mu m$  for low multiplicity pp events. The position of the pp collision is determined in 3 dimensions via the tracks reconstructed in the central tracker system. In low multiplicity pp events, the small number of tracks found in the ITS and the TPC leads to a broadening of the vertex resolution. In the extreme case, the event cannot be reconstructed in the central part of the detector because the position of the primary vertex is not well determined. In this study, a selection is therefore made to remove those pp events prior to strange particle analysis. Selected events are the ones where at least one SPD (Silicon Pixel Detector) tracklet [19, 20] has been found. The accuracy of some reconstruction parameters depends on the primary vertex reconstruction. The broadening of the primary vertex resolution translates therefore into a decrease of the efficiency. However, relaxing the selection parameters increases in the same time the efficiency and minimizes the sensitivity to the error on the primary vertex position. Designed primarily for the reconstruction of Pb–Pb collisions, ALICE is also perfectly able to deal with high multiplicity pp events. Thus, the efficiency is essentially improving for those events.

Table 1: pp events classes used for this analysis.

Events	double diffractive	single diffractive	non diffractive	total
not selected	9098	14451	3643	27192
selected (% triggered events)	9386 (4.3%)	12891 (5.1%)	101681 (90.6%)	123958

We generated minimum bias pp collisions with PYTHIA 6.214 tuned for the LHC [21]. Table 1 contains the numbers of events divided in non-diffractive, single and double diffractive processes. Approximately 82% of all generated events are selected for this study. However the event trigger would decrease this number. Assuming that a coincidence between both V0 detectors is required, the event trigger efficiency has been estimated to be 98% for non diffractive events, 50.7% for double diffractive events and 43.5% for single diffractive events [22]. The corresponding proportion in the analyzed event sample of each category when the trigger efficiency is taken into account is written in brackets in Table 1.

### 3 Single strange particle identification: $\Lambda$ and $K_S^0$

For pp events, the reconstruction of secondary  $V^0$  vertices is studied with two different selection samples listed in Table 2. The first sample corresponds to the selection parameters employed for the event reconstruction which is done prior to the analysis. At this level, the selections have to be as loose as possible in order to record, in the Event Summary Data (ESD) files, most of the secondary vertices whilst keeping the amount of background at a reasonable level. They have been chosen to set the memory size of the array of  $V^0$  vertices in those ESD files at approximately 1/15 of the size of the track array. For the second sample, tighter selections are applied so the purity is improved and we obtain approximately the S/B ratio required for typical spectra and correlation analysis.

Table 2: Selection parameters for strangeness reconstruction in pp events.  $b_-/b_+$  are the minimum impact parameters of the negative/positive track.  $\cos \Theta_{p\Lambda}$  is the pointing angle, i.e. the angle between the candidate momentum and the segment between the  $V^0$  vertex and the primary vertex. The daughter dca is the distance to closest approach of the two tracks forming up the  $V^0$  vertex. The decay length is the calculated value for each  $V^0$  candidate.

Selections	$b_-/b_+$ min. ( $\mu\text{m}$ )	$\cos \Theta_{p\Lambda}$ min.	daughter dca max. (cm)	decay length min. (cm)
loose	21	0.717	5.30	0.07
tight	115	0.994	3.46	0.34

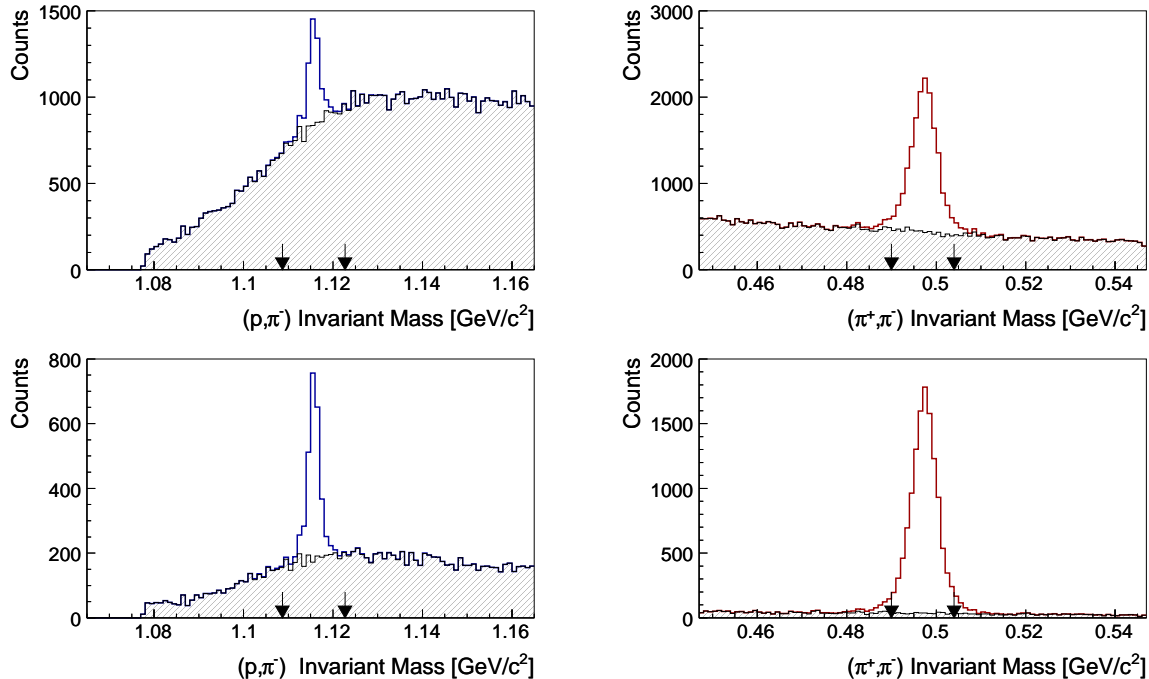


Figure 1: Invariant mass distributions of  $\Lambda$  and  $K_S^0$  candidates reconstructed in pp events for both loose (upper panels) and tight selections (lower panels).

The invariant mass distributions of  $\Lambda$  and  $K_S^0$  candidates are presented in Fig. 1. The upper panels of Fig. 1 show the signals and backgrounds for the first sample whereas the lower part shows the distributions from the second sample. The total integrated reconstruction rates for both  $\Lambda + \bar{\Lambda}$  and  $K_S^0$  are presented on the left panel of Fig. 2 for the second selection sample. The reconstruction rate, or global correction factor, is defined in this note as the probability to reconstruct a given particle and takes into account the acceptance, the efficiency and the decay channel probability. The maximum reconstruction rates are therefore equal to the decay channel probabilities. The upper part of the left panel shows the event distribution and the lower part the reconstruction rates, both as a function of the charged track multiplicity. A clear drop of the reconstruction rates appears at low multiplicity while they remain essentially constant after  $N_{ch} > 30$ . This decrease is mainly due to the softening of the momentum distribution of single strange particles in low multiplicity collisions. Indeed, as shown for the  $\Lambda$  on Fig. 3, the global correction factor of the strange particle increases gradually with  $p_t$  from 0 to 3 GeV/c and introduces a strong dependence between the momentum distribution and the reconstruction rate. The influence of the primary vertex resolution can be seen on the right part of Fig. 2 where the intrinsic efficiency (computed by dividing the amount of reconstructed secondary vertices by the number of vertices which can be found) is plotted as a function of the multiplicity. The efficiency is mainly constant for loose selections but starts to decrease for tight selection parameters and at low multiplicity. This behaviour can be explained by the fact that the  $V^0$  reconstruction becomes more sensitive to the precision of the measurement of the primary vertex position when the selections are tightened. Although the effect is weak, the analysis of pp events therefore requires the separation of events in multiplicity classes. We plan to investigate in detail this multiplicity dependence with high statistics. Nevertheless the reconstruction rate of  $\Lambda + \bar{\Lambda}$  as a function of  $p_t$  and for low ( $N_{ch} < 20$ ) and high ( $N_{ch} > 30$ ) multiplicity events can still be calculated (see the right panel of Fig. 3). No strong difference is found between the two distributions except a slightly lower reconstruction rate for low  $N_{ch}$ . Finally Fig. 4 shows an estimation of the raw  $\Lambda$  distribution versus  $p_t$  for one year of LHC pp runs (i.e.  $10^9$  events). This distribution is based on the  $\Lambda$  Monte Carlo production in PYTHIA minimum bias events which is fitted by an *ad hoc* function. The function is then corrected by the actual reconstruction rate of Fig. 3 and scaled by the expected number of events.

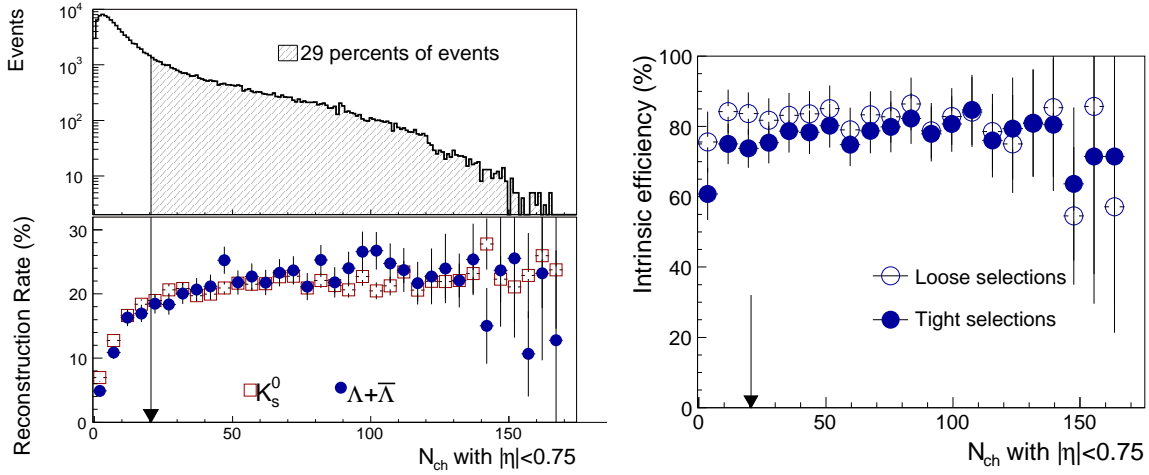


Figure 2: On the left panel, event distribution and reconstruction rate for  $\Lambda$  (open symbols) and  $K_S^0$  (full symbols) as a function of pp collision track multiplicity. On the right panel, intrinsic efficiency of the  $V^0$  finding method as a function of the event multiplicity for the two sets of selections.

## 4 Cascade particle identification: $\Xi$ and $\Omega$

The reconstruction of cascades is also investigated for two sets of selections: one with loose selections and one with tighter parameters. As shown on Fig. 5, the signal of  $\Xi^- + \bar{\Xi}^+$  is clearly visible for both loose (left panel) and tight (right panel) selections. The S/B ratio are respectively  $\sim 0.3$  and  $\sim 2.6$ . The dependence with the cascade momentum is studied by generating pp data samples enriched with high  $p_t$   $\Xi^-$  and  $\bar{\Xi}^+$ . The resulting reconstruction rate as a function of  $p_t$  and for the tight selection parameters is shown on the left panel

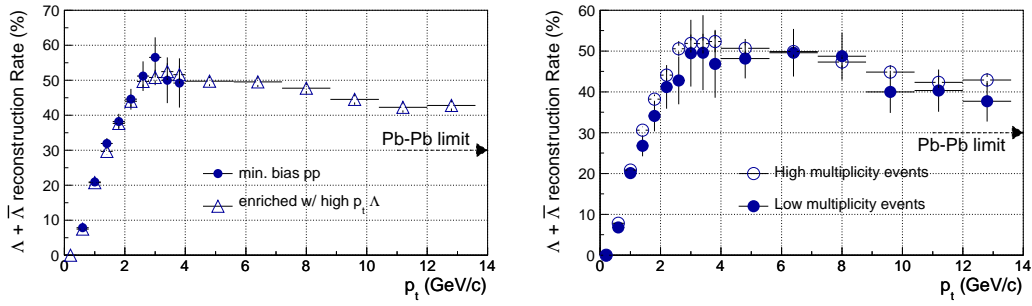


Figure 3: Reconstruction rate for  $\Lambda + \bar{\Lambda}$  as a function of  $p_t$ . On the left panel, the reconstruction rate is calculated for minimum bias pp events (full symbol) and for minimum bias events enriched in high  $p_t$   $\Lambda$  and  $\bar{\Lambda}$  (open symbol). On the right panel the reconstruction rates for low (full symbol) and for high (open symbol) multiplicity pp events are presented.

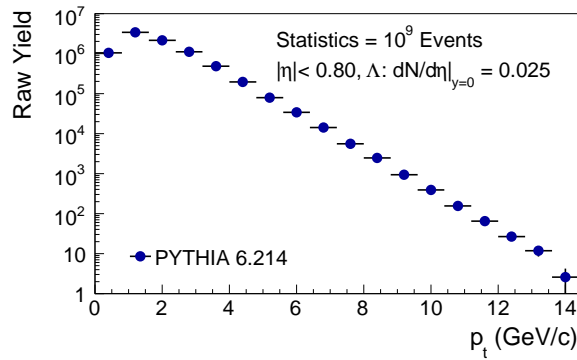


Figure 4: Distribution of reconstructed  $\Lambda$  as a function of  $p_t$  for  $10^9$  pp events at  $\sqrt{s} = 14$  TeV.

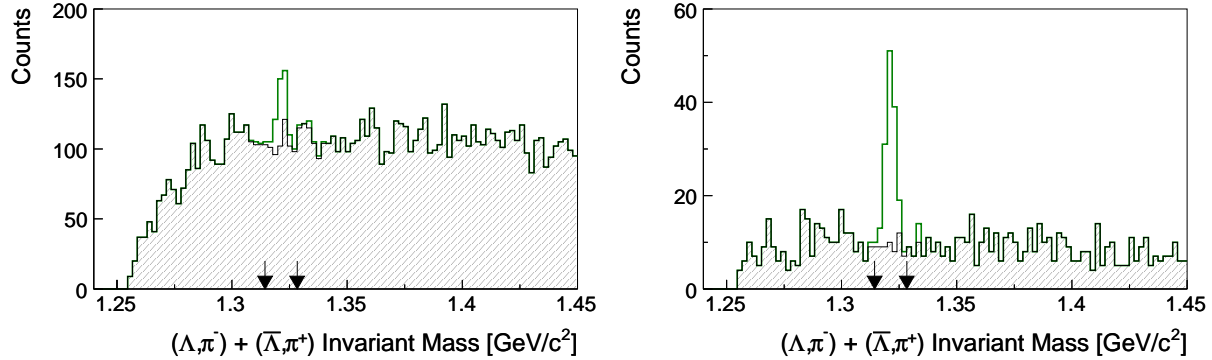


Figure 5: Invariant mass of  $\Xi^- + \bar{\Xi}^+$  candidates in pp events for loose (left panel) and tight (right panel) selections.

of Fig. 6 while the corresponding estimation of the reconstructed cascades distribution versus  $p_t$  is presented on the right.

In the case of  $\Omega$ , the reconstruction rate is estimated by scaling down the reconstruction rate of  $\Xi$  in pp collisions with the factor corresponding to the decrease of this rate for Pb–Pb collisions. Using the  $p_t$  distribution of the Monte Carlo  $\Omega$  generated with PYTHIA, we consequently estimate the reconstructed  $p_t$  distribution shown in Fig. 7.

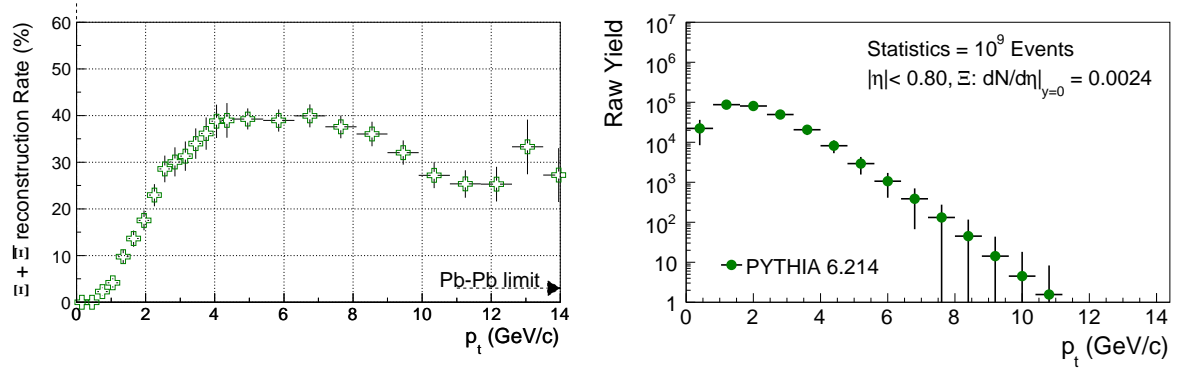


Figure 6: Left panel: Reconstruction rate of  $\Xi^- + \Xi^{-+}$ . Right panel: Estimated numbers of reconstructed  $\Xi^-$  for  $10^9$  pp events at  $\sqrt{s} = 14$  TeV as a function of  $p_t$ .

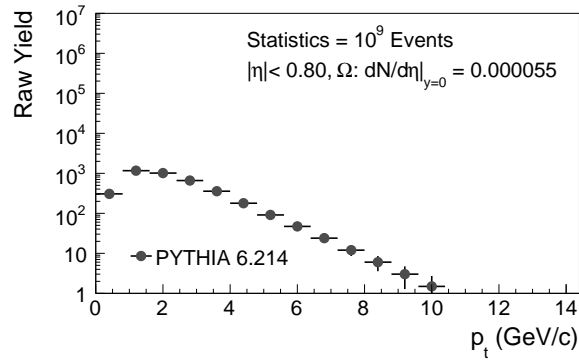


Figure 7: Distribution of reconstructed  $\Omega^-$  as a function of  $p_t$  for  $10^9$  pp events at  $\sqrt{s} = 14$  TeV.

## 5 Conclusion

Our preliminary studies of reconstruction rate and S/B show that a clean signal of all hyperons can be obtained in pp collisions during the first year of LHC operation. Not only this will allow to obtain the production yields with good accuracy (which is necessary for the feed down correction of lower mass particles) but it will be possible to investigate the shape of the spectra in detail. From the performed simulation and under the assumptions which were made, the  $p_t$  spectra should be available up to  $\sim 11$  GeV/c for  $\Lambda$ , up to  $\sim 8$  GeV/c for  $\Xi$  and up to  $\sim 5$  GeV/c for  $\Omega$ . Furthermore the events were generated with PYTHIA which tends to underestimate the yields for strange particles. Therefore the raw yields shown in this note may in reality have a better statistics and extend to higher transverse momenta. Moreover we expect to improve the reconstruction of strange secondary vertices by the development of advanced techniques of signal selection, which should be more efficient than the classical selections used in this note. The Linear Discriminant Analysis (LDA) has already shown a very good performance in the case of strange hyperon selection in ALICE [23].

## References

- [1] F. Carminati et al 2004 J. Phys. G **30** 1517-1763.
- [2] E. Andersen *et al.* (WA97 Collaboration), Phys. Lett. **B449** (1999) 401, L. Šandor *et al.* (NA57 Collaboration), J. Phys. G: Nucl. Part. Phys. **30** (2004) S129.
- [3] U. Heinz and M. Jacob, Preprint nucl-th/0002042.
- [4] J. Cleymans and K. Redlich, Phys. Rev. **C60** (1999) 054908; J. Cleymans, H. Oeschler and K. Redlich, Phys. Rev. **C59** (1999) 1663 and Phys. Lett. **B485** (2001) 27.
- [5] O. Fochler, S. Vogel, M. Bleicher, C. Greiner, P. Koch-Steinheimer and Z. Xu, Preprint hep-ph/0505025.
- [6] S. Hamieh, K. Redlich and A. Tounsi, Phys. Lett. **B486** (2000) 61.
- [7] H. Caines *et al.* (STAR Collaboration), J. Phys. G: Nucl. Part. Phys. **31** (2005) S1057.
- [8] T. Alexopoulos, et al., Phys. Lett. **B528** (2002) 43.
- [9] S.S. Adler *et al.* (PHENIX Collaboration), Phys. Rev. Lett. **91** (2003) 072303.
- [10] J. Adams *et al.* (STAR Collaboration), Phys. Rev. Lett. **91** (2003) 072304.
- [11] B. Z. Kopeliovich and B. G. Zakharov, Z. Phys. C **43** (1989) 241.
- [12] B. Kopeliovich and B. Povh, Phys. Lett. B **446** (1999) 321.
- [13] G. T. Garvey, B. Z. Kopeliovich and B. Povh, Comments Mod. Phys. A **2** (2001) 47.
- [14] R. Witt, J. Phys. G: Nucl. Part. Phys. **31** (2005) S863.
- [15] R. Bellwied, J. Phys. G: Nucl. Part. Phys. **31** (2005) S675.
- [16] M. Heinz, Preprint nucl-ex/0505025.
- [17] T. Sjöstrand, P. Edén, C. Friberg, L. Lönnblad, G. Miu, S. Mrenna and E. Norrbin, Computer Phys. Commun. 135 (2001) 238.
- [18] ALICE Collaboration, ALICE PPR vol. 2, to be published.
- [19] A. Badalà *et al.*, Internal Note ALICE-INT-2001-11.
- [20] N. Bustreo *et al.*, Internal Note ALICE-INT-2001-13.
- [21] ATLAS collaboration, phys-pub-2005-007, ATLAS note (2005).
- [22] M. Monteno, Private communication, 2005.
- [23] L. Gaudichet (ALICE Collaboration), Proceedings of the Hadron Collider Physics Symposium, Les Diablerets, Switzerland, July 4-9, 2005. To be published in EPJ.